THE JOURNAL OF BIOLOGICAL CHEMISTRY VOL. 287, NO. 31, pp. 25869–25880, July 27, 2012

Acetylation of Retinal Histones in Diabetes Increases Inflammatory Proteins

EFFECTS OF MINOCYCLINE AND MANIPULATION OF HISTONE ACETYLTRANSFERASE (HAT) AND HISTONE DEACETYLASE (HDAC)[*] [S]

Received for publication, April 27, 2012, and in revised form, May 30, 2012 Published, JBC Papers in Press, May 30, 2012, DOI 10.1074/jbc.M112.375204

Chandra Sekhar Rao Kadiyala[‡1,2], **Ling Zheng**[§1], **Yunpeng Du**[¶1], **Elizabeth Yohannes**[‡], **Hung-Ying Kao**[‖], **Masaru Miyagi**[‡‖**3,4], **and Timothy S. Kern**[¶‖**‡‡3,5]

From the [‡]*Case Center for Proteomics and Bioinformatics and Departments of* [¶]*Medicine,* [‖]*Biochemistry,* ***Ophthalmology and Visual Sciences, and* [‡‡]*Pharmacology, Case Western Reserve University, Cleveland, Ohio 441061 and the* [§]*College of Life Sciences, Wuhan University, Wuhan, China 430072*

Background: Processes that regulate inflammatory changes that contribute to the development of diabetic retinopathy are not known.
Results: Hyperglycemia increases histone acetylation, and HAT and HDAC inhibit this acetylation and induction of inflammatory proteins in retina.
Conclusion: Protein acetylation regulates the hyperglycemia-induced up-regulation of proinflammatory proteins.
Significance: Identification of acetylation as a regulator of proinflammatory processes in diabetes offers new therapeutic targets to inhibit the retinopathy.

Histone acetylation was significantly increased in retinas from diabetic rats, and this acetylation was inhibited in diabetics treated with minocycline, a drug known to inhibit early diabetic retinopathy in animals. Histone acetylation and expression of inflammatory proteins that have been implicated in the pathogenesis of diabetic retinopathy were increased likewise in cultured retinal Müller glia grown in a diabetes-like concentration of glucose. Both the acetylation and induction of the inflammatory proteins in elevated glucose levels were significantly inhibited by inhibitors of histone acetyltransferase (garcinol and antisense against the histone acetylase, p300) or activators of histone deacetylase (theophylline and resveratrol) and were increased by the histone deacetylase inhibitor, suberolylanilide hydroxamic acid. We conclude that hyperglycemia causes acetylation of retinal histones (and probably other proteins) and that the acetylation contributes to the hyperglycemia-induced up-regulation of proinflammatory proteins and thereby to the development of diabetic retinopathy.

Diabetic retinopathy is a major contributor to the morbidity and cost of diabetes, but its pathogenesis remains unclear. Several studies indicate that inflammatory proteins, such as ICAM-1,[6] VEGF, iNOS, and cytokines, play key roles in development of the retinopathy (1).

Post-translational modifications such as phosphorylation, acetylation, methylation, and ubiquitination regulate signal transduction pathways under normal conditions as well as in diseases such as diabetes (2). In chromatin, DNA base pairs are organized around core histones, and those histones are subject to multiple post-translational modifications that regulate many aspects of cell viability, including gene expression, apoptosis, and DNA replication and repair (3, 4). Dysregulation or unbalanced levels of histone modifications are involved in or associated with human diseases, including cancer, neurodegeneration, and inflammation (5, 6).

Histone acetylation and deacetylation are mediated by histone acetyltransferases (HATs) and histone deacetylases (HDACs), respectively. Acetylation of specific lysine residues on core histones is believed to result in uncoiling of the DNA and increased accessibility to transcription factor binding. When proinflammatory transcription factors, such as NF-κB, are activated, they bind to specific recognition sequences in DNA and then recruit coactivator molecules, such as p300, to the target gene promoters. These coactivator molecules control gene transcription, and most of them have intrinsic HAT activity (7, 8). In contrast, histone deacetylation mediates transcriptional repression by compacting chromatin, thereby limiting access to transcription factors. Thus, a balance between acetylation and deacetylation states of these proteins contributes to the regulation of transcription.

* This work was supported, in whole or in part, by National Institutes of Health Grant EY00300. This work was also supported by a merit grant from the Veterans Affairs (to T. S. K.), by Visual Sciences Research Center of Case Western Reserve University Grant P30EY-11373, and by funds from Case Western Reserve University and the Cleveland Foundation.
[S] This article contains supplemental Fig. S1, Table S1, Methods, Results, and additional references.
[1] These authors contributed equally to this work.
[2] Present address: Dept. of Cell Biology, Lerner Research Institute, Cleveland Clinic Foundation, Cleveland, OH 44195.
[3] Co-senior authors.
[4] To whom correspondence may be addressed: Case Center for Proteomics and Bioinformatics, Case Western Reserve University, 10900 Euclid Ave., Cleveland, OH 44106-4988. Tel.: 216-368–5917; Fax: 216-368-6846; E-mail: masaru.miyagi@case.edu.
[5] To whom correspondence may be addressed: Dept. of Medicine, Case Western Reserve University, 10900 Euclid Ave., Cleveland, OH 44106-4988. Tel.: 216-368-0800; Fax: 216-368-3419; E-mail: tsk@case.edu.

[6] The abbreviations used are: ICAM-1, intercellular adhesion molecule 1; HAT, histone acetyltransferase; HDAC, histone deacetylase; iNOS, inducible NOS; MS/MS, tandem MS; SAHA, suberolylanilide hydroxamic acid.

This report investigates the effect of diabetes and elevated glucose concentration on acetylation of retinal histones. Using Western blotting and mass spectroscopy, we find that diabetes and increased glucose concentration increase the acetylation at several lysine residues on histones. Hyperglycemia-induced acetylation regulates the induction of several proinflammatory proteins in retinas of hyperglycemic animals, and both acetylation and expression of the inflammatory proteins can be inhibited by manipulating HAT/HDAC activity or with minocycline (which inhibits early stages of diabetic retinopathy) (9–11).

EXPERIMENTAL PROCEDURES

Materials—H3K9 and H4K16 antibodies were purchased from Bachem Americas (Torrance, CA), and sequencing grade modified bovine trypsin was from Promega. $^{13}C_4$-acetic anhydride was purchased from Sigma-Aldrich. SDS-containing polyacrylamide gels were purchased from Bio-Rad. All other chemicals and materials used were either reagent grade or of the highest quality commercially available.

In Vivo Studies—Diabetes was induced in fasted male rats (Lewis) with streptozotocin as reported previously (12). Only rats with blood glucose higher than 250 mg/dl and glycated hemoglobin level above 8% were considered as diabetic. Rats were killed at 10 weeks after the onset of diabetes. Minocycline was administered to some diabetic animals at a dose of 10 mg/kg (intraperitoneal injection, 5× per week) for the duration of the study.

In Vitro Studies—Transformed retinal Müller (glial) cells (rMC-1 cell line) (13–16) were cultured and passaged in DMEM containing 5.5 mM glucose and 10% FBS. When cells were 70% confluent, the concentration of FBS in 5 or 30 mM glucose medium was reduced to 1–2%.

To manipulate protein acetylation in the rMC-1 cells, a HAT inhibitor (20 μM garcinol) (17), HDAC activators (10 μM theophylline) (18), and 50 μM resveratrol (19), and a broad spectrum HDAC inhibitor (1 μM suberolylanilide hydroxamic acid (SAHA)) (20) were added to the medium at published concentrations (listed above). Minocyline was administered to other rMC-1 cells at a dose of 20 nM (11). Theophylline, SAHA, and minocycline were administered for the full 4 days of incubation, whereas garcinol and resveratrol were administered only the final 24 h of the incubation.

p300 siRNA Transfection—To knock down expression of the HAT p300, siRNA against p300 (SC-29432) and inactive control siRNA (SC-37007, both from Santa Cruz Biotechnology, Santa Cruz, CA) were transfected into rMC-1 cells. The p300 siRNA was transfected using a X-tremeGENE siRNA Transfection Reagent (Roche Applied Science) according to the manufacturer's protocol. In brief, 6-well plates of rMC-1 cells were cultured to 80% confluence, and each well was incubated with 2 ml of antibiotic-free complete medium containing 100 μl if siRNA Transfection Reagent and 1.5 μg of either p300 siRNA or control siRNA. Experiments were performed 96 h after transfection.

Western Blot Analysis—Proteins were resolved by SDS-PAGE and probed with antibodies for histone H2A, histone H2B, histone H3, acetylhistone H2A, acetylhistone H2B, acetylhistone H3, acetylhistone H4 (1:1000 dilution; Cell Signaling Technology, Danvers, MA). The densitometry results of Western blots were expressed as the mean ± S.D. The data were analyzed by ANOVA followed by Fisher's post hoc test. Differences were considered statistically significant when $p < 0.05$.

Isolation, Purification, and S-Alkylation of Histones from Retinal Müller Cells—Cultured rMC-1 cells were incubated in medium containing 5, 30, or 30 mM glucose plus 5 μM minocycline. Histones from the groups were extracted and purified separately. Cells were treated with 5 ml of PBS containing protease inhibitors (1 mM EDTA, 0.2 mM PMSF, 0.7 μg/μl leupeptin, and 0.5 μg/μl pepstatin A), phosphatase inhibitor mixture 3 (Sigma), and HDAC inhibitors (5 mM nicotinamide and 1 μM trichostatin A) (3) for 5 min. Cells were scraped from the plate and lysed using a hand-held polypropylene pestle. For the non-gel-based mass spectroscopic (MS) studies, soluble proteins were extracted using 0.1 M sulfuric acid. The sulfuric acid-soluble fraction was further fractionated on an ion exchange column to further purify histones H3 and H4 (21). Histones were eluted from the ion exchange column using 2 ml of 1 M NaCl, pH adjusted to 8.0, and then the volume was reduced to 0.4 ml in a SpeedVac concentrator. Proteins were then reduced by 10 mM DTT at 37 °C for 1 h and *S*-alkylated using 25 mM iodoacetamide at 25 °C in the dark for 1 h (22). The reduced and *S*-alkylated proteins were desalted using a Vydac C18 MicroSpin column (The Nest Group, Southborough, MA) according to the manufacturer's instructions. The desalted histone proteins in 60% acetonitrile were dried in the SpeedVac and redissolved in 100 μl of water. Protein was quantified using the DC Protein assay kit (Bio-Rad).

Quantitation of Histone Acetylation by Non-gel-based MS—To quantitate the degree of acetylation of given amino acids, we chemically acetylated all histone ϵ-amino groups to completion using $^{13}C_4$-acetic anhydride and then compared the amount of chemical acetylation (^{13}C-acetyl) to the amount of endogenous acetylation (^{12}C-acetyl) on individual lysines. The chemical acetylation of histone ϵ-amino groups was carried out as described by Smith *et al.* (4) with a few modifications. We used $^{13}C_4$-acetic anhydride instead of D_6-acetic anhydride for the chemical acetylation because it results in the smaller mass shift from the endogenously acetylated species (2 Da instead of 3 Da). This makes it easier to subject equally both the chemically and endogenously acetylated species to tandem mass spectrometry (MS/MS), especially for peptides that have more than one lysine residue. Twenty-five μg of the purified histone was dissolved in 100 μl of 50 mM 4-ethylmorpholine acetic acid, pH 8, buffer containing 50% acetonitrile, and incubated with 10 mM $^{13}C_4$-acetic anhydride for 2 h, followed by treating with 100 mM hydroxylamine for 1 h to reverse the possible acylation on the cysteine sulfhydryl, tyrosine hydroxyl, and histidine imidazole groups. After the reaction, this reaction mixture was desalted using a Vydac C18 MicroSpin column, digested by trypsin in 25 mM ammonium bicarbonate, and analyzed by LC-MS/MS.

Proteins were identified by comparing all of the experimental peptide MS/MS spectra to the Rodent histone using Mascot data base search software (version 2.1.04; Matrix Science, London, UK). *S*-Carbamidomethylation of cysteine was set as a fixed modification whereas oxidation of methionine (methionine sulfoxide) and lysine $^{13}C_2$-acetyl modification were vari-

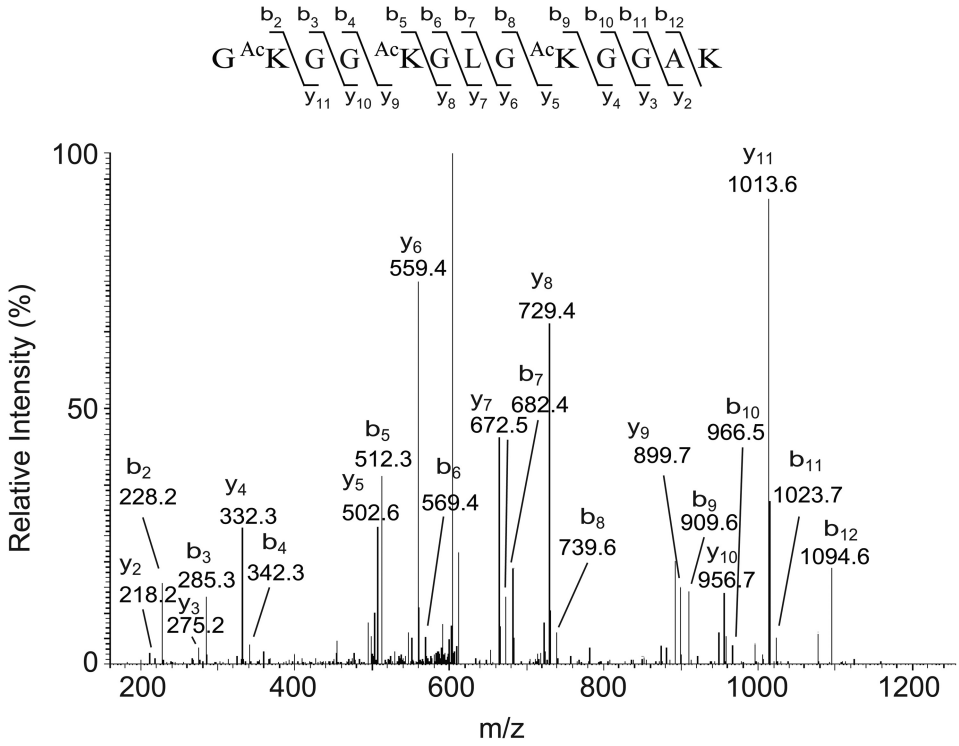

FIGURE 1. **MS/MS of the *m/z* 620.85 (+2 charge, spot 2305) precursor of the identified sequence residues 5–17, GKGGKGLGKGGAK, of histone H4.** Spot (master number 2305) was excised from a two-dimensional gel and subjected to in-gel tryptic digestion. A scheme summarizing the observed fragment ions of this peptide is shown above the mass spectrum.

able modifications. The mass tolerance for the precursor ion was set to 10 ppm, and the product ion was set to 0.1 Da. Strict trypsin specificity was applied, allowing for five missed cleavages. Only peptides with a minimum score of 20 or higher were considered significant. Peptide identifications were accepted if they could be established at an ion score greater than 30, as specified by the Peptide Prophet algorithm (23). Data analysis to calculate the extent of acetylation at individual sites from the mass spectrometry data is described in the supplemental Methods and Results.

RESULTS

In Vivo Studies of Acetylation—Two-dimensional difference gel electrophoresis analysis of retinal tissues from nondiabetic ($n = 4$) and diabetic animals ($n = 4$) revealed ~2300 protein spots per gel, and the mean intensities of 80 spots were significantly different in the retinas of diabetic rats compared with age-matched controls (data not shown). The subsequent LC-MS/MS analyses of these spots identified a total of 59 unique proteins (supplemental Table S1), some of which were found in multiple spots, suggesting post-translational modification.

Among all of the altered proteins in the retinas of diabetic rats, LC-MS/MS analysis revealed five different forms of histones in 12 differentially expressed spots as being especially altered in diabetic retinas. Although the theoretic pI values of the histones are very basic, the two-dimensional migration patterns demonstrated that the diabetes-induced alterations in spots that were identified as histones by MS/MS were located in neutral pH ranges. We speculated that post-translational modifications, such as lysine acetylation or arginine citrullination, could neutralize the positive charges and cause the pI shift of histones. Fig. 1 shows the MS/MS spectrum of a peptide from one spot with an apparent pI of ~7.3, which was identified as histone H4 peptide. The peptide GKGGKGLGKGGAK with the precursor m/z of 620.85 ($z = 2$) that matched histone H4 residues 4–16 (not including the initiator methionine as the first amino acid) was identified with acetylated lysines at positions 5, 8, and 12. An additional spectrum for the same spot identified another peptide GGKGLGKGGAKR that matched histone H4 residues 6–17 (precursor m/z of 606.34, $z = 2$) showing the acetylation at Lys^8, Lys^{12}, and Lys^{16} (data not shown). The intensity of this spot was 1.5-fold increased in retinas of diabetic rats *versus* nondiabetic rats, suggesting that acetylation of this specific histone isoform was increased in the retina in diabetes.

To confirm these findings, total and acetylated histone levels in the retinas were investigated by Western blotting (Fig. 2). Acetylated histone H2A, H2B, H3, and H4 were increased approximately 2-fold in the retinas of diabetic rats compared with those of the nondiabetic rats ($p < 0.05$), whereas total histone H2A, H2B, H3, and H4 expression levels were similar in the retinas of diabetic and nondiabetic rats. Minocycline, a drug known to inhibit early stages of diabetic retinopathy (10, 11), significantly inhibited the diabetes-induced acetylation of retinal histones H2, H3, and H4 (all $p < 0.05$).

In Vitro Studies of Acetylation—To investigate whether histones also became hyperacetylated in retinal cells cultured in diabetic-like concentrations of glucose, rMC-1 cells were used. After incubation in high glucose (30 mM) medium for 2–3 days,

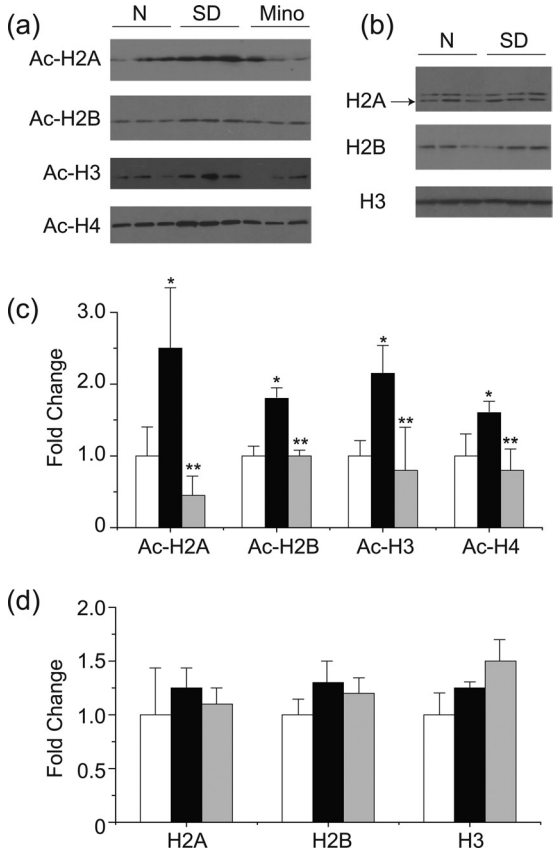

FIGURE 2. **Diabetes-induced increase in acetylated-histones in the retinas and inhibition of acetylation by minocycline.** Western blots of representative bands for specific acetylated histones and total histones are shown in *a* and *b*, respectively. Densitometric quantitation of results are summarized on *c* and *d*. Expression is relative to β-actin in same sample and normalized to nondiabetic retinas, set as 1-fold. *N*, nondiabetes; *SD*, diabetes. *, $p < 0.05$ compared with nondiabetes; **, $p < 0.05$ compared with diabetes.

the levels of acetylation on different lysines of histone H3 were evaluated by MS.

To quantitate the lysine acetylation, we chemically acetylated all available sites using $^{13}C_4$-acetic anhydride and then determined (by LC-MS/MS) how much of each potential acetylation site was occupied by enzymatic (endogenous) acetylation ($^{12}C_2$-acetyl) *versus* chemical acetylation ($^{13}C_2$-acetyl). We found three peptides whose acetylation appeared to be modulated by high glucose and/or minocycline.

The first peptide is histone H3 Lys^9-Arg^{17}. This peptide carries two lysine residues, H3K9 and H3K14. The isotope clusters of the peptide from different experimental groups (treated with 5 mM glucose, 30 mM glucose, and 30 mM glucose and minocycline) are shown in Fig. 3*a*. The doubly charged peaks *m*/*z* 493.3, 494.3, and 495.3 represent the peptide species that contain zero (both lysine residues are endogenously acetylated), one (one of the lysine residues is endogenously acetylated), and two $^{13}C_2$-acetyl groups (neither of the lysine residues is endogenously acetylated), respectively. It is apparent that the intensities of *m*/*z* 493.3 and 494.3 increased relative to that of *m*/*z* 495.3 upon high glucose treatment, and this increase is inhibited by minocycline. To determine the residue-specific fractional extent of acetylation, the peptide was subjected to MS/MS. A representative tandem mass spectrum (Fig. 3*b*) confirms the identity of the peptide. Many product ions that contain either Lys^9 or Lys^{14} were observed. Among these product ions, we chose b_3 and y_7 ions, which contain Lys^9 and Lys^{14}, respectively, to calculate the residue-specific fractional acetylation because the intensities of these product ions are higher than those of the others. Fig. 3*c* shows the isotope clusters of the b_3 and y_7 ions from the different experimental groups. For b_3 ion, only the chemically acetylated species (*m*/*z* 361.2) was observed in all the experimental conditions, indicating that the extent of endogenous acetylation at Lys^9 is below the detection limit. However, the intensity of endogenously acetylated Lys^{14} (*m*/*z* 728.4) was clearly detected in cells treated with 5 mM glucose, the intensity (*m*/*z* 728.4) was increased significantly ($p < 0.01$) in high glucose relative to that of chemically acetylated species (*m*/*z* 730.4), and this increase was inhibited by minocycline treatment ($p < 0.01$). The fractional extent of endogenous acetylation at H3K14 was calculated from the spectra and found to be 38.0, 48.9, and 35.0% in the cells treated with 5 mM glucose, 30 mM glucose, and 30 mM glucose with 5 μM minocycline, respectively. The changes in endogenous acetylation at Lys^{14} are shown by the bar graph (Fig. 3*d*) as well as in Table 1. Thus, this result indicates that the hyperacetylation of H3K14 is increased under the high glucose condition, and this increased acetylation was inhibited by the addition of 5 μM minocycline.

The second peptide is histone H3 Lys^{18}-Arg^{26}. This peptide also carries two lysine residues, H3K18 and H3K23. The isotope clusters of the peptide from different experimental conditions are shown in Fig. 4*a*. The doubly charged peaks *m*/*z* 535.8, 536.8, and 537.8 represent the peptide species that contain zero (both lysine residues are endogenously acetylated), one (one of the lysine residues is endogenously acetylated), and two $^{13}C_2$-acetyl groups (neither lysine residue is endogenously acetylated), respectively. The spectra suggest that the acetylation at one or both of H3K18 or H3K23 increased in 30 mM glucose, and the hyperacetylation is decreased by minocycline treatment. MS/MS analysis of the peptide produced a number of product ions that contain either Lys^{18} or Lys^{23} (Fig. 4*b*). Among them, b_3 (contains Lys^{18}) and y_7 (contains Lys^{23}) ions were chosen for further analysis to obtain the quantitative information on the residue-specific endogenous acetylation. The isotope clusters of these ions are shown in Fig. 4*c*, and the changes of endogenous acetylation at H3K18 and H3K23 are summarized in Fig. 4*d* and Table 1. The fractional extent of endogenous acetylation at H3K18 was increased significantly ($p < 0.01$) upon high glucose treatment (4.0% → 5.9%) and inhibited ($p < 0.05$) by minocycline treatment (5.9% → 4.4%). However, the fractional extent of endogenous acetylation at H3K18 was <6% in all the experimental conditions. The fractional extent of endogenous acetylation at H3K23 was increased significantly ($p < 0.01$) upon high glucose treatment (32.7% → 45.9%) and inhibited slightly ($p < 0.05$) by minocycline treatment (45.9% → 42.1%). This result indicates that H3K23 acetylation is increased in high glucose concentration, and minocycline partially inhibits this increase.

The third peptide is histone H4 Gly^4-Arg^{17}. The peptide carries four lysine residues, Lys^5, Lys^8, Lys^{12}, and Lys^{16}. The iso-

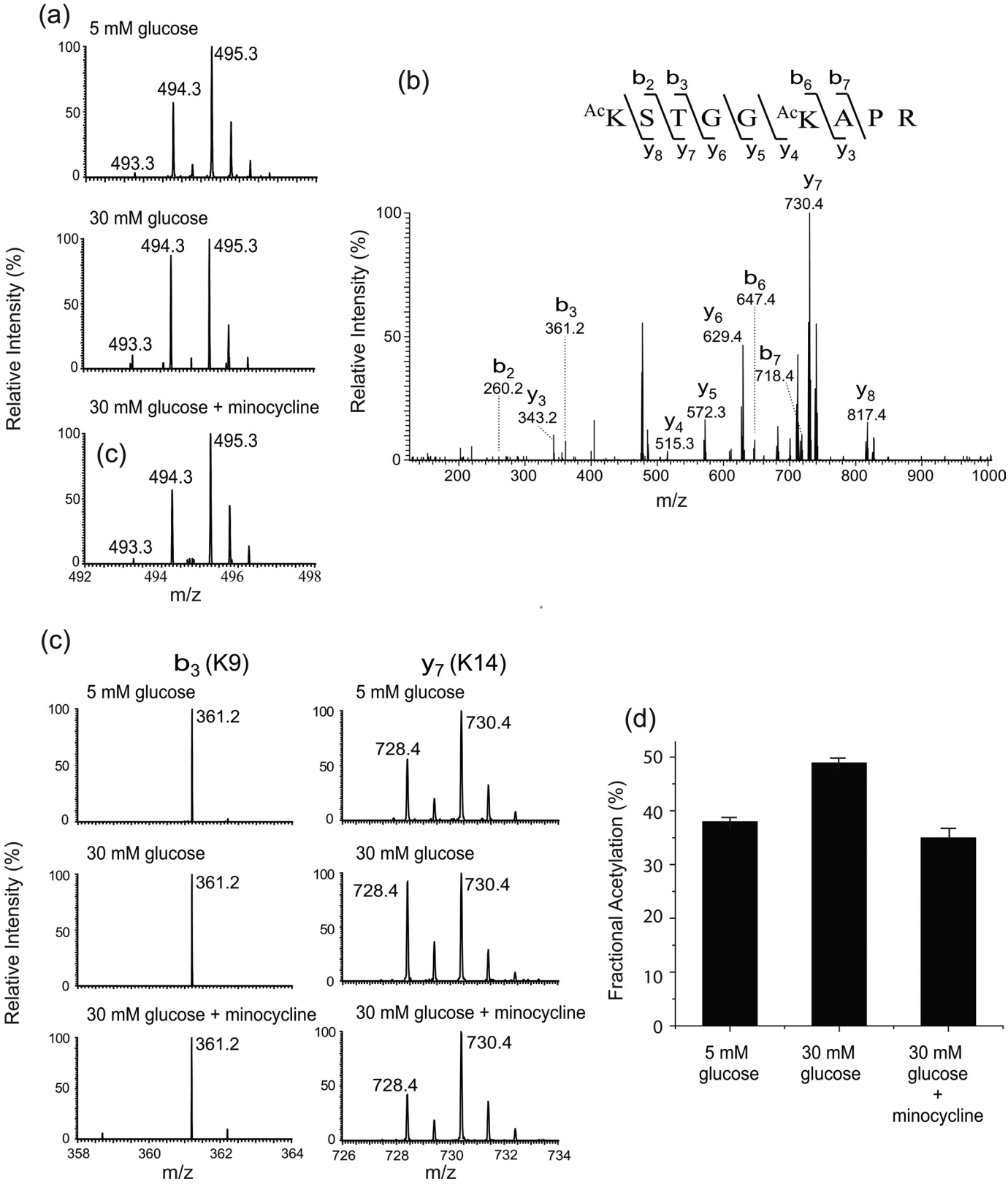

FIGURE 3. **Acetylation at H3K9 and H3K14.** *a*, mass spectra of a histone H3 peptide (Lys^9-Arg^{17}) from different experimental groups (treated with 5 mM glucose, 30 mM glucose, and 30 mM glucose and minocycline). The doubly charged peaks *m/z* 493.3, 494.3, and 495.3 represent the peptide species that carry two $^{12}C_2$-, one $^{12}C_2$- and one $^{13}C_2$-, and two $^{13}C_2$-acetyl groups, respectively. *b*, representative tandem mass spectrum of the peptide. *c*, close views of the singly charged b_3 and y_7 ions from the different experimental groups. The b_3 peak *m/z* 361.2 carries a $^{13}C_2$-acetyl group. The y_7 peaks *m/z* 728.4 and 730.4 carry a $^{12}C_2$- and $^{13}C_2$-acetyl group, respectively. *d*, changes of acetylation at H3K14.

TABLE 1
Fractional extent of endogenous histone acetylation in rMC-1 cells

Glucose	H3K9	H3K14	H3K18	H3K23	H4K5	H4K8	H4K12	H4K16
	%	%	%	%	%	%	%	%
5 mM	0.0	38.0 (±1.2)	4.0 (±0.4)	32.7 (±1.0)	0.0	12.9 (±0.9)	4.0 (±1.6)	34.6 (±1.6)
30 mM	0.0	48.9 (±1.3)[a]	5.9 (±0.4)[a]	45.9 (±0.7)[a]	7.8 (±3.6)[b]	11.9 (±4.2)	6.2 (±0.9)	51.7 (±2.1)[a]
30 mM +minocycline	0.0	35.0 (±4.3)[c]	4.4 (±0.8)[c]	42.1 (±1.4)[c]	5.0 (±2.4)	11.6 (±2.2)	5.3 (±1.0)	40.8 (±1.5)[d]

[a] $p < 0.01$ *vs.* 5 mM glucose.
[b] $p < 0.05$ *vs.* 5 mM glucose.
[c] $p < 0.01$ *vs.* 30 mM glucose.
[d] $p < 0.05$ *vs.* 30 mM glucose.

tope clusters of the peptide from different experimental conditions are shown in Fig. 5*a*. The doubly charged peaks *m*/*z* 719.9, 720.9, 721.9, 722.9, and 723.9 represent the peptide species that contain zero (all four lysine residues are endogenously acetylated), one (one of the lysine residues is endogenously acetylated), two (two of the lysine residues are endogenously acetylated), three (three of the lysine residues are endogenously acetylated), and four $^{13}C_2$-acetyl groups (neither of the lysine residues is endogenously acetylated), respectively. The spectra suggest that the acetylation at one or more of the lysine residues are increased upon high glucose treatment, and this hyperacetylation is decreased by minocycline. A representative tandem mass spectrum of the peptide is shown in Fig. 5*b*. We observed several product ions that contain a single lysine residue, either Lys^5 or Lys^{16}. We chose b_3 and y_5 ions to determine the fractional extent of endogenous acetylation at Lys^5 and Lys^{16}, respectively. The isotope clusters of the two ions are shown in Fig. 5*c*, and the changes in endogenous acetylation at Lys^5 and Lys^{16} are summarized in Fig. 5*d* and Table 1. The acetylation at Lys^5 was not observed in the cells treated with 5 mM glucose; however, it was detectable (7.8%) in the 30 mM glucose-treated cells. The inhibition of acetylation (7.8% → 5.0%) on Lys^5 by minocycline was not statistically significant. On the other hand, the fractional extent of endogenous acetylation at Lys^{16} was 34.6, 51.7, and 40.8% in cells treated with 5 mM glucose, 30 mM glucose, and 30 mM glucose with 5 μM minocycline, respectively, indicating an increase in acetylation upon high glucose treatment ($p < 0.01$) and an inhibition of the hyperacetylation by minocycline ($p < 0.01$). Because ions that contain only Lys^8 or Lys^{12} were not observed, it was not possible to determine the extent of endogenous acetylation at these sites straightforwardly. To determine the fractional extent of endogenous acetylation at Lys^8, we used a b_5 ion that contains Lys^5 and Lys^8 (Fig. 5*c*), and having the predetermined fractional extent of *in vivo* acetylation value at Lys^5, the fractional extent of endogenous acetylation at Lys^8 was estimated as described in the supplemental Methods and Results. The result is shown in Fig. 5*d* and Table 1. The fractional extent of endogenous acetylation was in the range of 11–13% in all of the experimental groups, and the changes were not statistically significant. Similarly, we used the b_7 ion that contains Lys^{12} and Lys^{16} (Fig. 5*c*) to determine the fractional extent of endogenous acetylation at Lys^{12}. The result indicates that the fractional extent of acetylation at this site was low (4–6.2%) in all of the experimental groups, and the changes were not statistically significant (Fig. 3*d* and Table 1).

Regulation of Histone Acetylation and Inflammatory Protein Expression by HAT Inhibitors and HDAC Activators and Inhibitor—rMC-1 cells were incubated in high glucose in the presence of activators or inhibitors of HATs and HDACs. As shown in Fig. 6*a*, garcinol (a HAT inhibitor), and resveratrol and theophylline (HDAC activators) significantly inhibited the acetylation of histone H3 caused by high glucose. These data suggest that hyperglycemia significantly enhances histone H3 acetylation in rMC-1 cells and does so via increased activity of HAT or reduced activity of HDAC. Because none of these agents is highly specific, however, we also tested the effect of siRNA against p300 HAT and the selective HDAC inhibitor, SAHA, on the acetylation. Knockdown of p300 significantly inhibited the glucose-induced acetylation of histone H3, and inhibition of HDACs with SAHA enhanced the hyperglycemia-induced acetylation of H3 (Fig. 6*b*). These data confirm that hyperglycemia enhances histone H3 acetylation in rMC-1 cells.

To explore the link between hyperglycemia-induced acetylation of retinal proteins and development of a proinflammatory state, we assessed the effect of the same HAT inhibitors, HDAC activators, and HDAC inhibitors on expression of ICAM-1, iNOS, and VEGF in rMC-1 cells. As can be seen in Fig. 7, garcinol, resveratrol, and theophylline significantly inhibited expression of iNOS, ICAM-1, and in most aspects, also VEGF in 30 mM glucose (Fig. 7, *a*–*d*). Moreover, antisense against p300 (but not an inactive control) significantly inhibited expression of ICAM (Fig. 7*e*), providing strong evidence that acetylation is important in the hyperglycemia-induced up-regulation of proinflammatory molecules in this retinal cell type. These *in vitro* studies are consistent with *in vivo* studies because the dose of minocycline that inhibited histone acetylation in retinas of diabetic rats likewise significantly inhibited the diabetes-induced increase in expression of ICAM-1 (Fig. 7*f*).

DISCUSSION

Histone acetylation and deacetylation play critical roles in the regulation of chromatin structure, which affects gene expression, DNA replication and repair, and chromosome condensation and segregation (24). Acetylation of histones confers accessibility of the DNA template to the transcriptional machinery for gene expression. Removal of acetyl groups from lysine residues in the N-terminal tail of histones, on the other hand, catalyzes and acts as transcriptional silencers of genes (25–27). Several disease conditions have been found to manifest alterations in post-translational modifications of histones and other proteins, suggesting that these modifica-

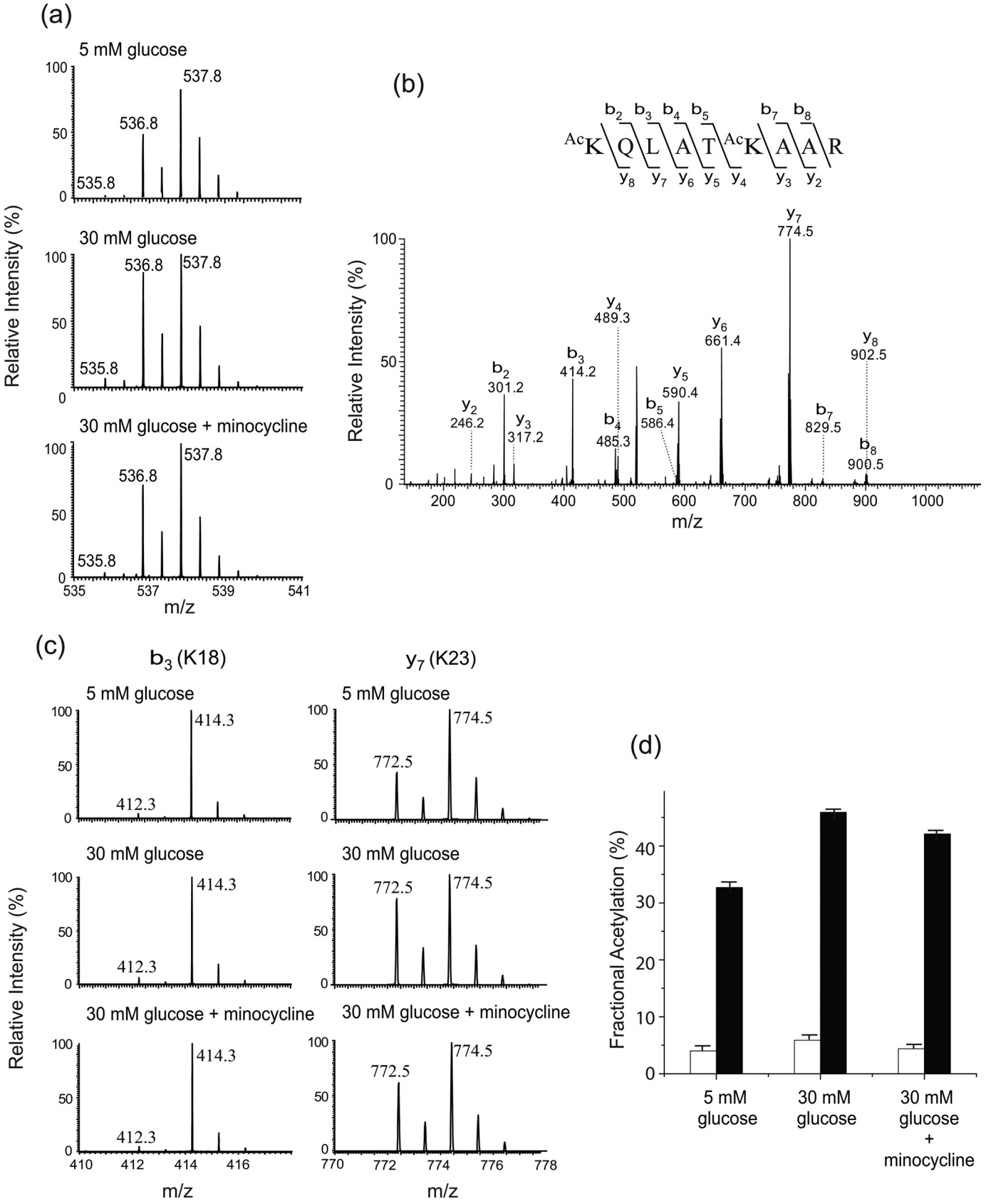

FIGURE 4. **Acetylation at H3K18 and H3K23.** *a*, mass spectra of a histone H3 peptide (Lys[18]-Arg[26]) from different experimental groups (treated with 5 mM glucose, 30 mM glucose, and 30 mM glucose and minocycline). The doubly charged peaks *m/z* 535.8, 536.8, and 537.8 represent the peptide species that carry two $^{12}C_2$-, one $^{12}C_2$- and one $^{13}C_2$-, and two $^{13}C_2$-acetyl groups, respectively. *b*, representative tandem mass spectrum of the peptide. *c*, close views of the singly charged b_3 and y_7 ions from the different experimental groups. The b_3 peaks *m/z* 412.3 and 414.3 carry a $^{12}C_2$- and $^{13}C_2$-acetyl group, respectively. The y_7 peaks *m/z* 772.5 and 774.5 carry a $^{12}C_2$- and $^{13}C_2$-acetyl group, respectively. *d*, changes of acetylation at H3K18 and H3K23.

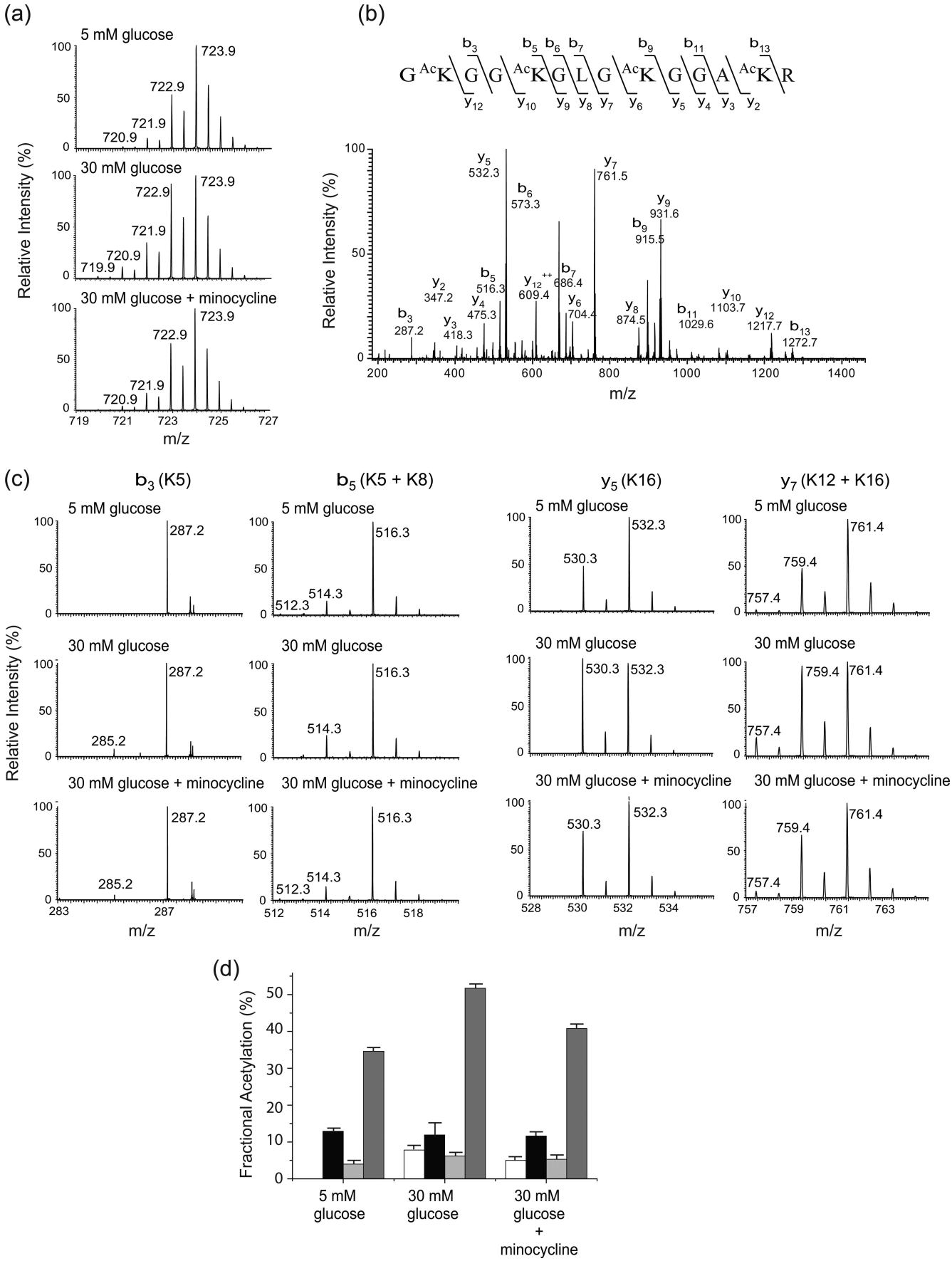
(a)
5 mM glucose
30 mM glucose
30 mM glucose + minocycline
Relative Intensity (%)
m/z
(b)
Relative Intensity (%)
m/z
(c)
b3 (K5)
b5 (K5 + K8)
y5 (K16)
y7 (K12 + K16)
5 mM glucose
30 mM glucose
30 mM glucose + minocycline
Relative Intensity (%)
m/z
(d)
Fractional Acetylation (%)
5 mM glucose
30 mM glucose
30 mM glucose + minocycline

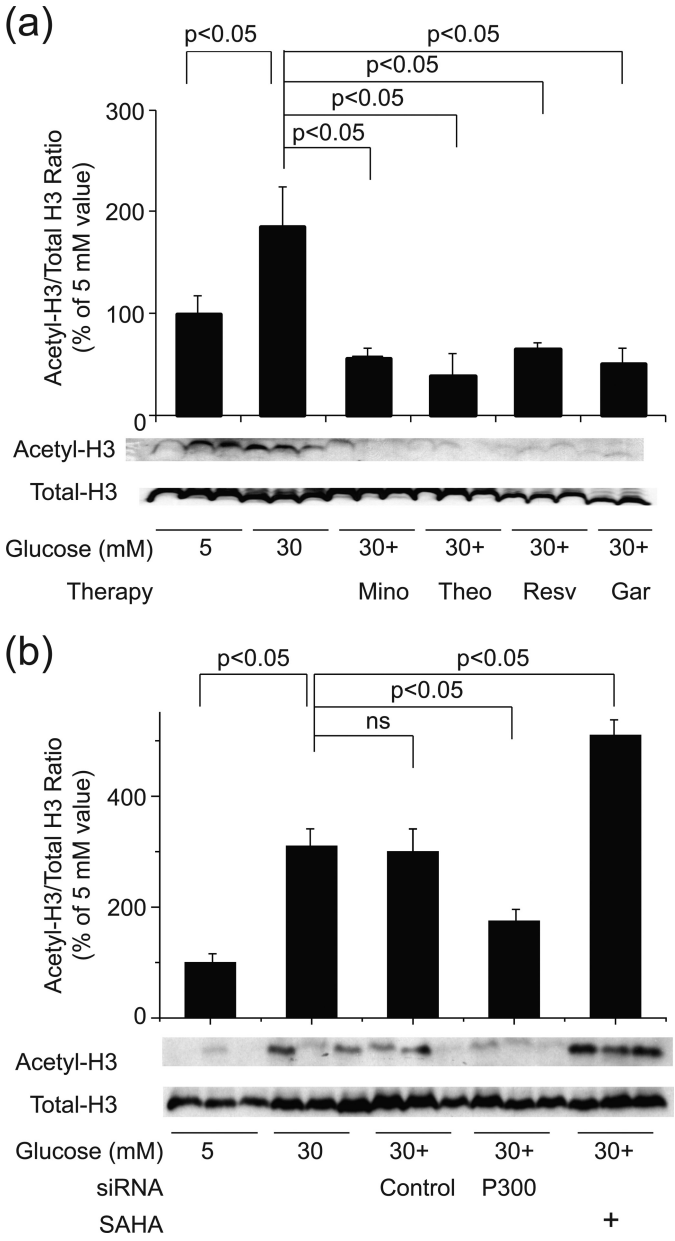

FIGURE 6. **Regulation of histone H3 acetylation by manipulating HAT or HDAC.** *a*, incubation of rMC-1 cells in 30 mM glucose led to a significant increase in histone H3 acetylation, and this was inhibited by a HAT inhibitor (garcinol (*Gar*)), by HDAC activators (theophylline (*Theo*) and resveratrol (*Resv*)), and by minocycline (*Mino*). *b*, likewise, the increased acetylation of histone H3 in high glucose was inhibited by siRNA against p300 but not by an inactive control. Acetylation of histones was increased above normal in cells grown with the HDAC inhibitor, SAHA. The data in both figures summarize results from six dishes and Western blot data from three representative dishes.

tions might contribute to the development of cellular pathology.

Diabetes, likewise, alters acetylation patterns in a variety of tissues, with the majority of studies showing that diabetes increases histone acetylation. Natarajan and colleagues showed that diabetes or elevated glucose concentration led to increased acetylation of lysines on histones H3 (at Lys^9 and Lys^{14}) and H4 (at Lys^5, Lys^8, and Lys^{12}) on monocytes, and increased transcription of TNFα and COX2 (28). Moreover, overexpression of histone deacetylase inhibited, and a HDAC inhibitor stimulated, histone acetylation and transcription of TNFα in these cells. Yun *et al.* (6) detected similar changes in monocytes from diabetic patients. Perrone *et al.* (29) likewise found that incubation of retinal endothelial cells in high glucose increased acetylation of histone H3, and increased histone acetylation was detected at H3K9 and H3K23 in type 2 diabetic mice showing evidence of diabetic kidney disease or hearts of mice undergoing renal failure (30, 31). The present studies demonstrate that experimental diabetes led to increases in histone H3 and H4 acetylation in retina, and incubation of retinal Müller glial cells in hyperglycemia-like conditions resulted in a similar significant increase in acetylation of histone H3.

In contrast, some other studies have reported decreased histone acetylation in diabetes, with histone acetylation being subnormal in retina (32) and kidney (33). We cannot explain these prior results but note that they used only antibody-based methods to assess acetylation. Our MS approaches clearly demonstrate that acetylation of retinal histones is increased by experimentally diabetic animals and that acetylation on specific lysine residues of H3 and H4 can be modulated by high glucose and minocycline. In tissue samples, however, the MS methods did not always confirm the antibody-based Western blots. Western blots of retinas from diabetic animals indicated that H3K9 acetylation was increased by 2-fold, but this was not confirmed using MS/MS.

A close relationship between histone acetylation and inflammatory gene transcription has been observed. Histone deacetylase inhibitors have been reported to enhance inflammatory gene transcription in a number of cell lines (34–36). In addition, NF-κB-dependent transcription of inflammatory genes such as COX-2 and iNOS is regulated by HATs and by HDACs (35–39). Our data using siRNA against the HAT p300 indicate that acetylation clearly is involved in the increased transcription of some inflammatory proteins in response to elevated glucose, thus confirming that this relationship between acetylation and expression of proinflammatory proteins holds also in retinal cells exposed to hyperglycemia.

Several studies found that acetylation of specific lysine residues in histones is responsible for proinflammatory molecule induction. Jeong *et al.* found acetylation of histone H3K9 and H3K14 in lipopolysaccharide (LPS)-treated macrophage cell line (RAW264.7 cells), leading to induction of nitric oxide, PGE_2, and expression of iNOS and COX-2 (40). Chung and colleagues found that the acetylation of histone H3K9 recruited NF-κB inducing kinase to promoters of proinflammatory genes

FIGURE 5. **Acetylation at H4K5, H4K8, H4K12, and H4K16.** *a*, mass spectra of a histone H4 peptide (Gly^4-Arg^{17}) from different experimental groups (treated with 5 mM glucose, 30 mM glucose and 30 mM glucose, and minocycline). The doubly charged peaks *m/z* 719.9, 720.9, 721.9, 722.9, and 723.9 represent the peptide species that carry four $^{12}C_2$-, three $^{12}C_2$- and one $^{13}C_2$-, two $^{12}C_2$- and two $^{13}C_2$-, one $^{12}C_2$- and three $^{13}C_2$-, and four $^{13}C_2$-acetyl groups, respectively. *b*, representative tandem mass spectrum of the peptide. *c*, close views of the singly charged b_3, b_5, y_5, and y_7 ions from the different experimental groups. The b_3 peaks *m/z* 285.2 and 287.2 carry a $^{12}C_2$- and $^{13}C_2$-acetyl group, respectively. The b_5 peaks *m/z* 512.3, 514.3, and 516.3 carry two $^{12}C_2$-, one $^{12}C_2$- and one $^{13}C_2$-, and two $^{13}C_2$-acetyl groups, respectively. The y_5 peaks *m/z* 530.3 and 532.3 carry a $^{12}C_2$- and $^{13}C_2$-acetyl group, respectively. The y_7 peaks *m/z* 757.4, 759.4, and 761.4 carry two $^{12}C_2$-, one $^{12}C_2$- and one $^{13}C_2$-, and two $^{13}C_2$-acetyl groups, respectively. *d*, changes of acetylation at H4K5, H4K8, H4K12, and H4K16.

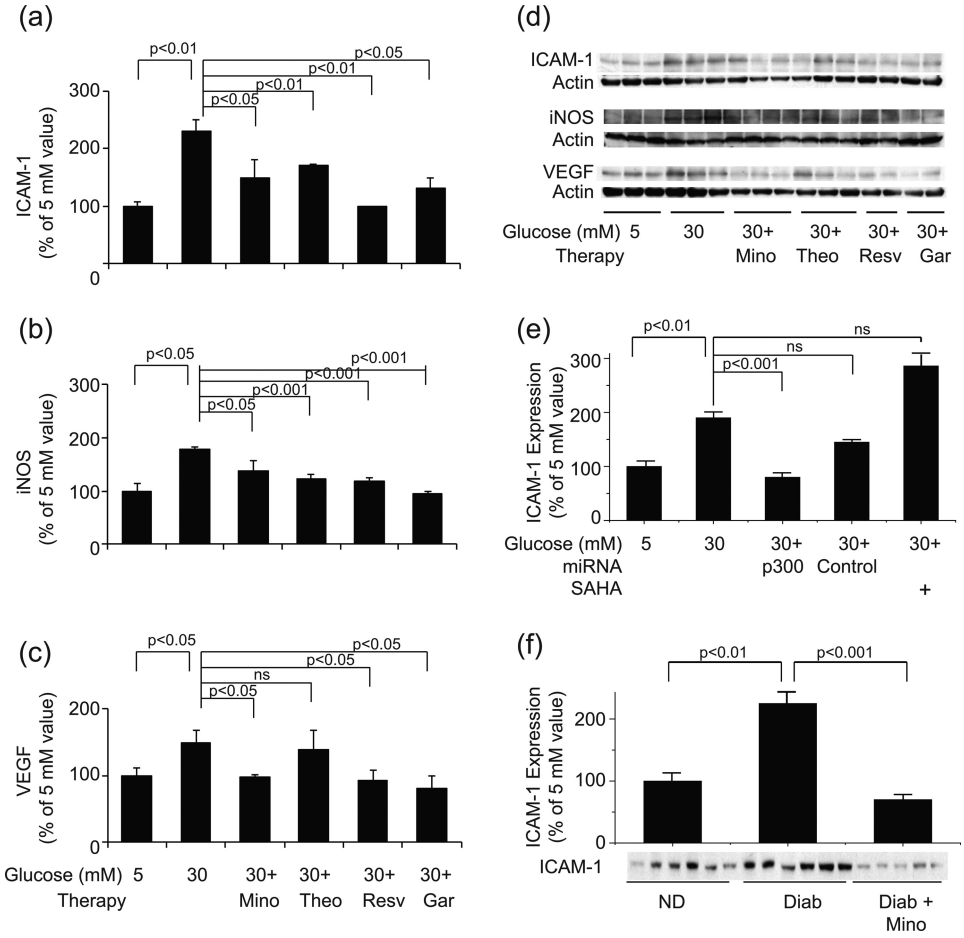

FIGURE 7. *a–c*, expression of the proinflammatory proteins, ICAM-1 (*a*), iNOS (*b*), and VEGF (*c*) by rMC-1 cells incubated in 5 or 30 mM glucose for 4 days. HAT inhibitors and HDAC activators were added to some samples. The graphical data in the figures summarize data from six dishes. *d*, representative results from Western blotting, with data from three representative dishes shown. *e*, siRNA against p300 decreasing, and inhibition of HDAC using SAHA increasing, expression of ICAM-1. The graphical data in the figures summarize data from six dishes. *f*, retinas from diabetic mice treated with minocycline for 2 months likewise showing a significant reduction in retinal expression of ICAM-1 compared with untreated diabetics ($n = 6$ per group). *ns*, not statistically significant. Other abbreviations are as in Fig. 6.

such as IL-6, IL-8, and COX-2 (41, 42). Morinobu *et al.* showed that acetylation of histone H3K9, H3K8, and H4K12 contributes to the preferential induction of IFN-γ and T-bet genes in T helper cells (43). These results support the hypothesis that acetylation of histones participates in the regulation of inflammatory responses. We found increased acetylation on histone H3K14, H3K18, H3K23, H4K5, and H4K16 in rMC-1 cells in high glucose and modulation of some of those sites (H3K14, H3K18, H3K23, and H4K16) by minocycline. These changes appeared to be positively correlated with the inductions of proinflammatory molecules (ICAM, iNOS, and VEGF). Although we have provided evidence that acetylation regulates expression of inflammatory proteins, it is not yet clear whether the acetylation specifically of histones or non-histone proteins (such as promoters for the various inflammatory proteins) is important (28, 44–46).

Many of the molecular and physiologic abnormalities that have been found to develop in the retina in diabetes are consistent with inflammation, and pharmacologic inhibition or genetic deletion of proinflammatory enzymes inhibits development of the early stages of the retinopathy in animals (1). For example, diabetes causes induction of iNOS and ICAM in the retina, and deficiency of either enzyme inhibits the diabetes-induced degeneration of retinal capillaries that is characteristic of the retinopathy (47, 48). The beneficial effect of intravitreal corticosteroids against diabetic macular edema (49–52) suggests that inflammatory pathways play a role also in advanced diabetic retinopathy in patients. Corticosteroids are among the strongest anti-inflammatory agents known and mediate this anti-inflammatory effect at least in part by inhibiting histone acetylation (53, 54).

Minocycline previously has been shown to inhibit early stages of diabetic retinopathy in animal models (10, 11), but the mechanism of this action has not been known. Our data suggest that inhibition of diabetes-induced increases in acetylation and inflammation might be one such mechanism. Poorly specific modifiers of histone acetylation, such as theophylline (18), garcinol, and resveratrol, likewise inhibit the acetylation, and thus we predict that they also could inhibit the inflammatory changes that contribute to development of the retinopathy. The demonstration that acetylation in elevated glucose regulates expression of inflammatory proteins in retinal cells further suggests that acetylation contributes to the pathogenesis of diabetic retinopathy. Thus, pharmacologic inhibition of that acetylation might be a novel therapeutic target to inhibit development of the retinopathy.

REFERENCES

1. Tang, J., and Kern, T. S. (2011) Inflammation in diabetic retinopathy. *Prog. Retin. Eye Res.* **30,** 343–358
2. Mukherji, M. (2005) Phosphoproteomics in analyzing signaling pathways. *Expert Rev. Proteomics* **2,** 117–128
3. Guan, K. L., Yu, W., Lin, Y., Xiong, Y., and Zhao, S. (2010) Generation of acetyllysine antibodies and affinity enrichment of acetylated peptides. *Nat. Protoc.* **5,** 1583–1595
4. Smith, C. M., Gafken, P. R., Zhang, Z., Gottschling, D. E., Smith, J. B., and Smith, D. L. (2003) Mass spectrometric quantification of acetylation at specific lysines within the amino-terminal tail of histone H4. *Anal. Biochem.* **316,** 23–33
5. Kazantsev, A. G., and Thompson, L. M. (2008) Therapeutic application of histone deacetylase inhibitors for central nervous system disorders: nature reviews. *Drug Discovery* **7,** 854–868
6. Yun, J. M., Jialal, I., and Devaraj, S. (2011) Epigenetic regulation of high glucose-induced proinflammatory cytokine production in monocytes by curcumin. *J. Nutr. Biochem.* **22,** 450–458
7. Ogryzko, V. V., Schiltz, R. L., Russanova, V., Howard, B. H., and Nakatani, Y. (1996) The transcriptional coactivators p300 and CBP are histone acetyltransferases. *Cell* **87,** 953–959
8. Roth, S. Y., Denu, J. M., and Allis, C. D. (2001) Histone acetyltransferases. *Annu. Rev. Biochem.* **70,** 81–120
9. Bhatt, L. K., and Addepalli, V. (2010) Attenuation of diabetic retinopathy by enhanced inhibition of MMP-2 and MMP-9 using aspirin and minocycline in streptozotocin-diabetic rats. *Am. J. Transl. Res.* **2,** 181–189
10. Vincent, J. A., and Mohr, S. (2007) Inhibition of caspase-1/interleukin-1β signaling prevents degeneration of retinal capillaries in diabetes and galactosemia. *Diabetes* **56,** 224–230
11. Krady, J. K., Basu, A., Allen, C. M., Xu, Y., LaNoue, K. F., Gardner, T. W., and Levison, S. W. (2005) Minocycline reduces proinflammatory cytokine expression, microglial activation, and caspase-3 activation in a rodent model of diabetic retinopathy. *Diabetes* **54,** 1559–1565
12. Zheng, L., Howell, S. J., Hatala, D. A., Huang, K., and Kern, T. S. (2007) Salicylate-based anti-inflammatory drugs inhibit the early lesion of diabetic retinopathy. *Diabetes* **56,** 337–345
13. Du, Y., Sarthy, V. P., and Kern, T. S. (2004) Interaction between NO and COX pathways in retinal cells exposed to elevated glucose and retina of diabetic rats. *Am. J. Physiol. Regul. Integr. Comp. Physiol.* **287,** R735–741
14. Du, Y., Smith, M. A., Miller, C. M., and Kern, T. S. (2002) Diabetes-induced nitrative stress in the retina, and correction by aminoguanidine. *J. Neurochem.* **80,** 771–779
15. Sarthy, V. P., Brodjian, S. J., Dutt, K., Kennedy, B. N., French, R. P., and Crabb, J. W. (1998) Establishment and characterization of a retinal Müller cell line. *Invest. Ophthalmol. Vis. Sci.* **39,** 212–216
16. Shelton, M. D., Kern, T. S., and Mieyal, J. J. (2007) Glutaredoxin regulates nuclear factor κB and intercellular adhesion molecule in Müller cells: model of diabetic retinopathy. *J. Biol. Chem.* **282,** 12467–12474
17. Balasubramanyam, K., Altaf, M., Varier, R. A., Swaminathan, V., Ravindran, A., Sadhale, P. P., and Kundu, T. K. (2004) Polyisoprenylated benzophenone, garcinol, a natural histone acetyltransferase inhibitor, represses chromatin transcription and alters global gene expression. *J. Biol. Chem.* **279,** 33716–33726
18. Ito, K., Lim, S., Caramori, G., Cosio, B., Chung, K. F., Adcock, I. M., and Barnes, P. J. (2002) A molecular mechanism of action of theophylline: induction of histone deacetylase activity to decrease inflammatory gene expression. *Proc. Natl. Acad. Sci. U.S.A.* **99,** 8921–8926
19. Huang, C., Ma, W. Y., Goranson, A., and Dong, Z. (1999) Resveratrol suppresses cell transformation and induces apoptosis through a p53-dependent pathway. *Carcinogenesis* **20,** 237–242
20. Butler, L. M., Zhou, X., Xu, W. S., Scher, H. I., Rifkind, R. A., Marks, P. A., and Richon, V. M. (2002) The histone deacetylase inhibitor SAHA arrests cancer cell growth, up-regulates thioredoxin-binding protein-2, and down-regulates thioredoxin. *Proc. Natl. Acad. Sci. U.S.A.* **99,** 11700–11705
21. Rodriguez-Collazo, P., Leuba, S. H., and Zlatanova, J. (2009) Robust methods for purification of histones from cultured mammalian cells with the preservation of their native modifications. *Nucleic Acids Res.* **37,** e81
22. Rao, K. C., Palamalai, V., Dunlevy, J. R., and Miyagi, M. (2005) Peptidyl-Lys metalloendopeptidase-catalyzed ^{18}O labeling for comparative proteomics: application to cytokine/lipolysaccharide-treated human retinal pigment epithelium cell line. *Mol. Cell. Proteomics* **4,** 1550–1557
23. Keller, A., Nesvizhskii, A. I., Kolker, E., and Aebersold, R. (2002) Empirical statistical model to estimate the accuracy of peptide identifications made by MS/MS and database search. *Anal. Chem.* **74,** 5383–5392
24. Verdone, L., Agricola, E., Caserta, M., and Di Mauro, E. (2006) Histone acetylation in gene regulation. *Brief Funct. Genomic Proteomic* **5,** 209–221
25. Wade, P. A. (2001) Transcriptional control at regulatory checkpoints by histone deacetylases: molecular connections between cancer and chromatin. *Hum. Mol. Genet.* **10,** 693–698
26. de Ruijter, A. J., van Gennip, A. H., Caron, H. N., Kemp, S., and van Kuilenburg, A. B. (2003) Histone deacetylases (HDACs): characterization of the classical HDAC family. *Biochem. J.* **370,** 737–749
27. Saha, R. N., and Pahan, K. (2006) HATs and HDACs in neurodegeneration: a tale of disconcerted acetylation homeostasis. *Cell Death Differ.* **13,** 539–550
28. Miao, F., Gonzalo, I. G., Lanting, L., and Natarajan, R. (2004) *In vivo* chromatin remodeling events leading to inflammatory gene transcription under diabetic conditions. *J. Biol. Chem.* **279,** 18091–18097
29. Perrone, L., Devi, T. S., Hosoya, K., Terasaki, T., and Singh, L. P. (2009) Thioredoxin interacting protein (TXNIP) induces inflammation through chromatin modification in retinal capillary endothelial cells under diabetic conditions. *J. Cell. Physiol.* **221,** 262–272
30. Sayyed, S. G., Gaikwad, A. B., Lichtnekert, J., Kulkarni, O., Eulberg, D., Klussmann, S., Tikoo, K., and Anders, H. J. (2010) Progressive glomerulosclerosis in type 2 diabetes is associated with renal histone H3K9 and H3K23 acetylation, H3K4 dimethylation and phosphorylation at serine 10. *Nephrol. Dial. Transplant.* **25,** 1811–1817
31. Gaikwad, A. B., Sayyed, S. G., Lichtnekert, J., Tikoo, K., and Anders, H. J. (2010) Renal failure increases cardiac histone H3 acetylation, dimethylation, and phosphorylation and the induction of cardiomyopathy-related genes in type 2 diabetes. *Am. J. Pathol.* **176,** 1079–1083
32. Zhong, Q., and Kowluru, R. A. (2010) Role of histone acetylation in the development of diabetic retinopathy and the metabolic memory phenomenon. *J. Cell. Biochem.* **110,** 1306–1313
33. Tikoo, K., Meena, R. L., Kabra, D. G., and Gaikwad, A. B. (2008) Change in post-translational modifications of histone H3, heat-shock protein-27, and MAP kinase p38 expression by curcumin in streptozotocin-induced type I diabetic nephropathy. *Br. J. Pharmacol.* **153,** 1225–1231
34. Chen, H., Tini, M., and Evans, R. M. (2001) HATs on and beyond chromatin. *Curr. Opin. Cell Biol.* **13,** 218–224
35. Ito, T., Ikehara, T., Nakagawa, T., Kraus, W. L., and Muramatsu, M. (2000) p300-mediated acetylation facilitates the transfer of histone H2A-H2B dimers from nucleosomes to a histone chaperone. *Genes Dev.* **14,** 1899–1907
36. Ashburner, B. P., Westerheide, S. D., and Baldwin, A. S., Jr. (2001) The p65 (RelA) subunit of NF-κB interacts with the histone deacetylase (HDAC) corepressors HDAC1 and HDAC2 to negatively regulate gene expression. *Mol. Cell. Biol.* **21,** 7065–7077
37. Sheppard, K. A., Rose, D. W., Haque, Z. K., Kurokawa, R., McInerney, E., Westin, S., Thanos, D., Rosenfeld, M. G., Glass, C. K., and Collins, T. (1999) Transcriptional activation by NF-κB requires multiple coactivators. *Mol. Cell. Biol.* **19,** 6367–6378
38. Deng, W. G., Zhu, Y., and Wu, K. K. (2004) Role of p300 and PCAF in regulating cyclooxygenase-2 promoter activation by inflammatory mediators. *Blood* **103,** 2135–2142
39. Yu, Z., Zhang, W., and Kone, B. C. (2002) Histone deacetylases augment cytokine induction of the iNOS gene. *J. Am. Soc. Nephrol.* **13,** 2009–2017
40. Jeong, J. B., Hong, S. C., Jeong, H. J., and Koo, J. S. (2011) Anti-inflammatory effect of 2-methoxy-4-vinylphenol via the suppression of NF-κB and MAPK activation, and acetylation of histone H3. *Arch. Pharm. Res.* **34,** 2109–2116
41. Chung, S., Sundar, I. K., Hwang, J. W., Yull, F. E., Blackwell, T. S., Kinnula, V. L., Bulger, M., Yao, H., and Rahman, I. (2011) NF-κB-inducing kinase, NIK, mediates cigarette smoke/TNFα-induced histone acetylation and

inflammation through differential activation of IKKs. *PLoS One* **6,** e23488
42. Yang, S. R., Valvo, S., Yao, H., Kode, A., Rajendrasozhan, S., Edirisinghe, I., Caito, S., Adenuga, D., Henry, R., Fromm, G., Maggirwar, S., Li, J. D., Bulger, M., and Rahman, I. (2008) IKKα causes chromatin modification on proinflammatory genes by cigarette smoke in mouse lung. *Am. J. Respir. Cell Mol. Biol.* **38,** 689–698
43. Morinobu, A., Kanno, Y., and O'Shea, J. J. (2004) Discrete roles for histone acetylation in human T helper 1 cell-specific gene expression. *J. Biol. Chem.* **279,** 40640–40646
44. Shanmugam, N., Reddy, M. A., Guha, M., and Natarajan, R. (2003) High glucose-induced expression of proinflammatory cytokine and chemokine genes in monocytic cells. *Diabetes* **52,** 1256–1264
45. Li, Y., Reddy, M. A., Miao, F., Shanmugam, N., Yee, J. K., Hawkins, D., Ren, B., and Natarajan, R. (2008) Role of the histone H3 lysine 4 methyltransferase, SET7/9, in the regulation of NF-κB-dependent inflammatory genes: relevance to diabetes and inflammation. *J. Biol. Chem.* **283,** 26771–26781
46. Miao, F., Smith, D. D., Zhang, L., Min, A., Feng, W., and Natarajan, R. (2008) Lymphocytes from patients with type 1 diabetes display a distinct profile of chromatin histone H3 lysine 9 dimethylation: an epigenetic study in diabetes. *Diabetes* **57,** 3189–3198
47. Joussen, A. M., Poulaki, V., Le, M. L., Koizumi, K., Esser, C., Janicki, H., Schraermeyer, U., Kociok, N., Fauser, S., Kirchhof, B., Kern, T. S., and Adamis, A. P. (2004) A central role for inflammation in the pathogenesis of diabetic retinopathy. *FASEB J.* **18,** 1450–1452
48. Zheng, L., Du, Y., Miller, C., Gubitosi-Klug, R. A., Ball, S., Berkowitz, B. A., and Kern, T. S. (2007) Critical role of inducible nitric-oxide synthase in degeneration of retinal capillaries in mice with streptozotocin-induced diabetes. *Diabetologia* **50,** 1987–1996
49. Blumenkranz, M. S. (2010) Optimal current and future treatments for diabetic macular oedema. *Eye* **24,** 428–434
50. Schwartz, S. G., and Flynn, H. W., Jr. (2011) Fluocinolone acetonide implantable device for diabetic retinopathy. *Curr. Pharm. Biotechnol.* **12,** 347–351
51. Yilmaz, T., Cordero-Coma, M., Lavaque, A. J., Gallagher, M. J., and Padula, W. V. (2011) Triamcinolone and intraocular sustained-release delivery systems in diabetic retinopathy. *Curr. Pharm. Biotechnol.* **12,** 337–346
52. Yilmaz, T., Weaver, C. D., Gallagher, M. J., Cordero-Coma, M., Cervantes-Castaneda, R. A., Klisovic, D., Lavaque, A. J., and Larson, R. J. (2009) Intravitreal triamcinolone acetonide injection for treatment of refractory diabetic macular edema: a systematic review. *Ophthalmology* **116,** 902–911; quiz 912–913
53. Barnes, P. J. (2006) How corticosteroids control inflammation: Quintiles Prize Lecture 2005. *Br. J. Pharmacol.* **148,** 245–254
54. Barnes, P. J. (2011) Biochemical basis of asthma therapy. *J. Biol. Chem.* **286,** 32899–32905